© 2021 Wiley-VCH GmbH

ADVANCED FUNCTIONAL MATERIALS

Supporting Information

for *Adv. Funct. Mater.,* DOI: 10.1002/adfm.202105302

Universal Patterning for 2D Van der Waals Materials via Direct Optical Lithography

Seong Rae Cho, Seonghun Ahn, Seung Hyung Lee, Heonhak Ha, Tae Soo Kim, Min-kyung Jo, Chanwoo Song, Tae Hong Im, Pragya Rani, Minseung Gyeon, Kiwon Cho, Seungwoo Song, Min Seok Jang, Yong-Hoon Cho,* Keon Jae Lee,* and Kibum Kang**

© 2021 Wiley-VCH GmbH

Supporting Information

Universal patterning for 2D van der Waals Materials via direct optical lithography

Seong Rae Cho, Seonghun Ahn, Seung Hyung Lee, Heonhak Ha, Tae Soo Kim, Chanwoo Song, Tae Hong Im, Pragya Rani, Minseung Gyeon, Kiwon Cho, Min Seok Jang, Yong-Hoon Cho*, Keon Jae Lee*, Kibum Kang**

S1. Characterization of vdW materials

Raman spectroscopy and photoluminescence characterization were examined to confirm growth of ML MoS_2 and ML WSe_2. Raman spectrum of MoS_2, the red plot in Figure S1a, exhibited peaks at 386 cm^{-1} and 407 cm^{-1}, corresponding to characteristic peaks of MoS_2 and Raman spectrum of WSe_2, the green plot in Figure S1a, exhibited peaks at 250 cm^{-1}, corresponding to characteristic peaks of WSe_2. PL spectra in Figure S1b exhibited 670 nm and 750 nm in red and green plots, respectively, corresponding to those of ML MoS_2 and ML Wse_2.[s1]. How well graphene and MOF were prepared was examined by Raman spectroscopy. In Figure S2, graphene exhibited G band and 2D band peaks at 1564 cm^{-1} and 2677 cm^{-1}, respectively.[s2] In Figure S3, MOF exhibited several peaks which are identical with its characteristic peaks.[s3] BL MoS_2 was characterized by ellipsometry. Thickness of BL MoS_2 on 300-nm-thick SiO_2 was measured to be ~ 1.2 nm, which was identical with thickness of BL MoS2 in reference.[s4]

S2. Optical property variation before and after CP patterning

Despite the fact that the Raman spectra shows no significant changes of strain and defect density, optical properties of MoS_2 are modified. Therefore, we need to identify the origins of the changes after CP process, especially related to PR residues.

Absorption peaks of CP MoS_2 are all red-shifted after CP process compare to as-grown MoS_2. Meanwhile, the previous study reported that optical bandgap as well as exciton binding energy of ML MoS_2 on substrate with graphene on top decreased by reduced coulomb interaction.[22] Considering that CP MoS_2 sample was partially coated with photoresist residues as shown in AFM results (Figure 3a), the red shift is attributed to the modification of coulomb interaction by ultra-thin photoresist residues. The gradual increase of absorption as energy increases and local maximum at 3.5 eV are considered as the absorption of photoresist

itself, which was identified by measuring absorption of photoresist film sample without MoS_2 (Figure S9).

PL intensity decreases with three times amount after CP process compare to as-grown MoS_2. Generally, the PL intensity of semiconductors decreases if non-radiative recombination becomes dominant. In ML MoS2, there are two main causes of increased non-radiative recombination: Shockley-Read-Hall (SRH) effect, which is the trap-assisted non-radiative recombination from the extra state originated from various defect states, and Auger effect originated from high equilibrium electron density from natural doping.[s5,s6] For SRH effect, the density of defects should increase during the CP method, compared to the DOL method. However, it was revealed that the number of defects did not increase rapidly after the patterning processing in Raman spectra of Figure 3b. Meanwhile, it has been reported that the optical characteristics may vary depending on the type and pressure of the surrounding atmosphere.[s7,s8] CVD-grown MoS_2 generally has defect sites, considered as sulfur vacancies with low formation energy compared to the other sites.[s9] Electro-negative molecules such as O_2, H_2O in the air are physisorbed to the defect sites of MoS_2 with van der Waals interaction, inducing the decrease of equilibrium electron density in intrinsic areas, so called charge neutralization. Such an effect was reported to increase PL intensity of slightly defective MoS_2 by decreasing Auger non-radiative recombination effect.[s10] CP MoS_2 has photoresist residues on its surface as identified by AFM topography results (Figure 3a). They may have blocked the interaction between the defect sites and air molecules, so that they did not experience effective charge neutralization compared to as-grown MoS_2. Consequently, the PL intensity decreased in the CP sample. In contrast, DOL MoS_2 has no residues on its surface, so molecules in the air could still interact with exposed defect sites. Therefore, the PL intensity remains unchanged after patterning in ambient conditions.

To clarify the origin of red-shift of energy band and to exclude possible sample-to-sample variation, we directly compared optical signals before and after the CP process (Figure S10).

As a result, we found that both absorption and PL peaks are red-shifted after the CP process. Moreover, PL intensity decreases after the CP process, which is consistent with our observation as show in Fig. 3.

References

[s1] M. Yang, X. Cheng, Y. Li, Y. Ren, M. Liu, Z. Qi, *Appl. Phys. Lett.* **2017**, 110, 093108

[s2] G. Wang, B. Zhang, H. Ji, X. Liu, T. He, L. Lv, Y. Hou, J. Shen, *Appl. Phys. Lett.* **2017**, 110, 023301

[s3] J. M. S. Lopes, R. N. Sampaio, A. S. Ito, A. A. Batista, A. E. H. Machado, P. T. Araujo, N. M. Barbosa Neto, Spectrochim. Acta A Mol. Biomol. Spectrosc. *SPECTROCHIM ACTA A* **2019**, 215, 327

[s4] A. Zobel, A. Boson, P. M. Wilson, D. S. Muratov, D. V. Kuznetsov, A. Sintskii, *J. Mater. Chem. C* **2016**, 4, 11081

[s5] W. Siiocklev, A. W. T. Read, *Phys. Rev.* **1952**, 87, 807

[s6] A. Hangleiter, *Phys. Rev. B* **1988**, 37, 2594

[s7] S. Tongay, J. Zhou, C. Ataca, J. Liu, J. S. Kang, T. S. Matthews, L. You, J. Li, J. C. Gr ossman, J. Wu, *Nano Lett.* **2013**, 13, 2831.

[s8] S. Tongay, J. Suh, C. Ataca, W. Fan, A. Luce, J. S. Kang, J. Liu, C. Ko, R. Raghunath anan, J. Zhou, F. Ogletree, J. Li, J. C. Grossman, J. Wu, *Sci Rep* **2013**, 3, 2657.

[s9] S. Kc, R. C. Longo, R. M. Wallace, K. Cho, *J. Appl. Phys.* **2015**, 117, 135301.

[s10] D.-H. Lien, Z. Uddin, M. Yeh, M. Amani, H. Kim, J. W. A. Iii, E. Yablonovitch, A. Ja vey, *Science* **2019**, 364, 468

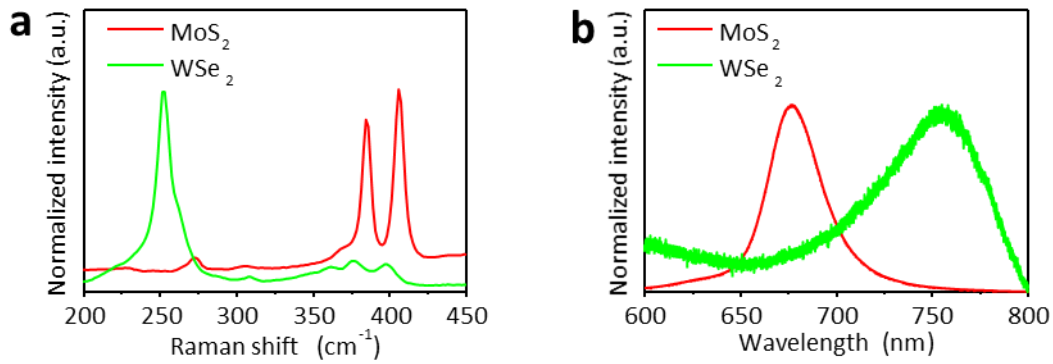

Figure S1. a, Normalized Raman spectra of MoS_2 and WSe_2, and **b**, normalized PL spectra of MoS_2 and WSe_2.

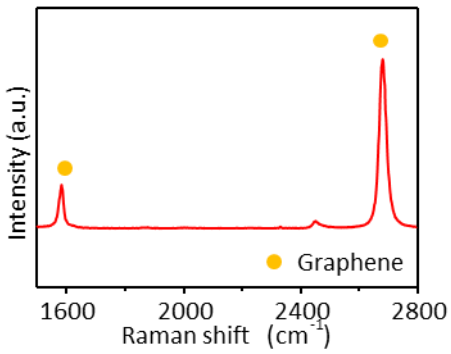

Figure S2. Raman spectrum of graphene.

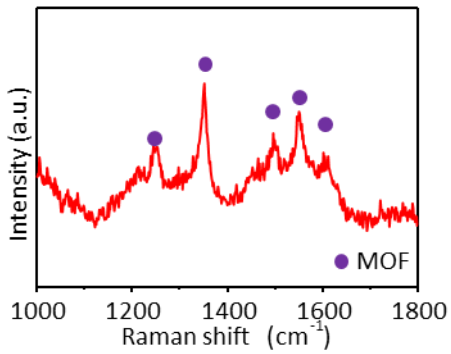

Figure S3. Raman spectrum of MOF.

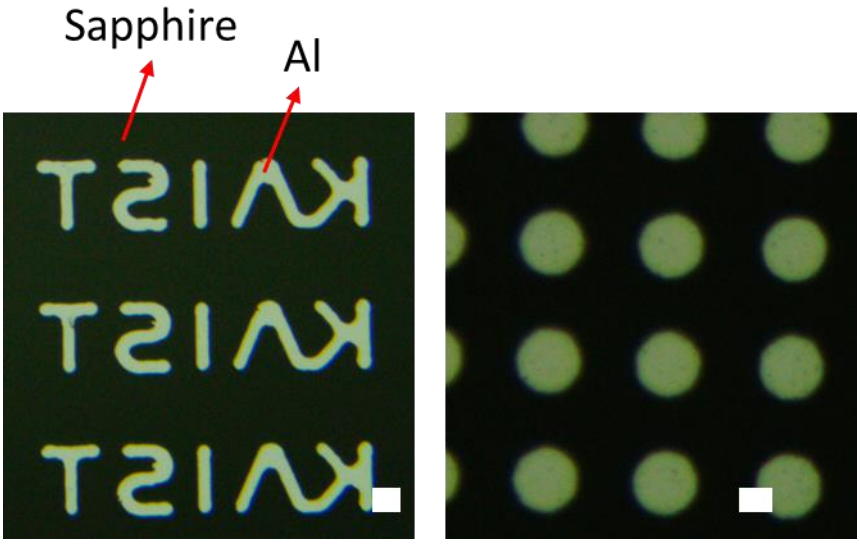

Figure S4. OM images on sapphire masks with a scale bar of 10 μm.

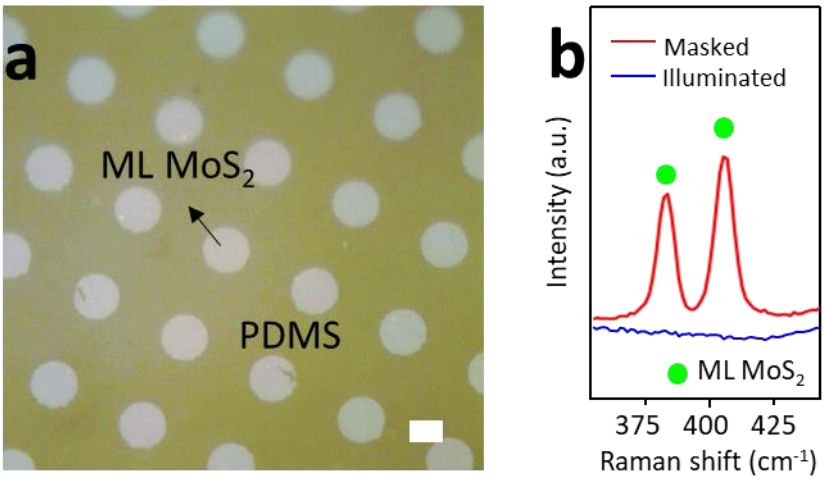

Figure S5. a, **b**, OM image (**a**) and Raman spectra (**b**) of patterned monolayer MoS_2 on a PDMS with a scale bar of 10 μm.

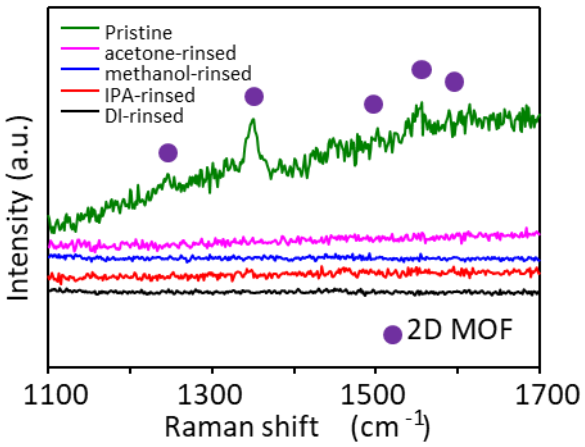

Figure S6. Raman spectra of pristine MOF, and MOF after rinsing in acetone, methanol, IPA, and DI.

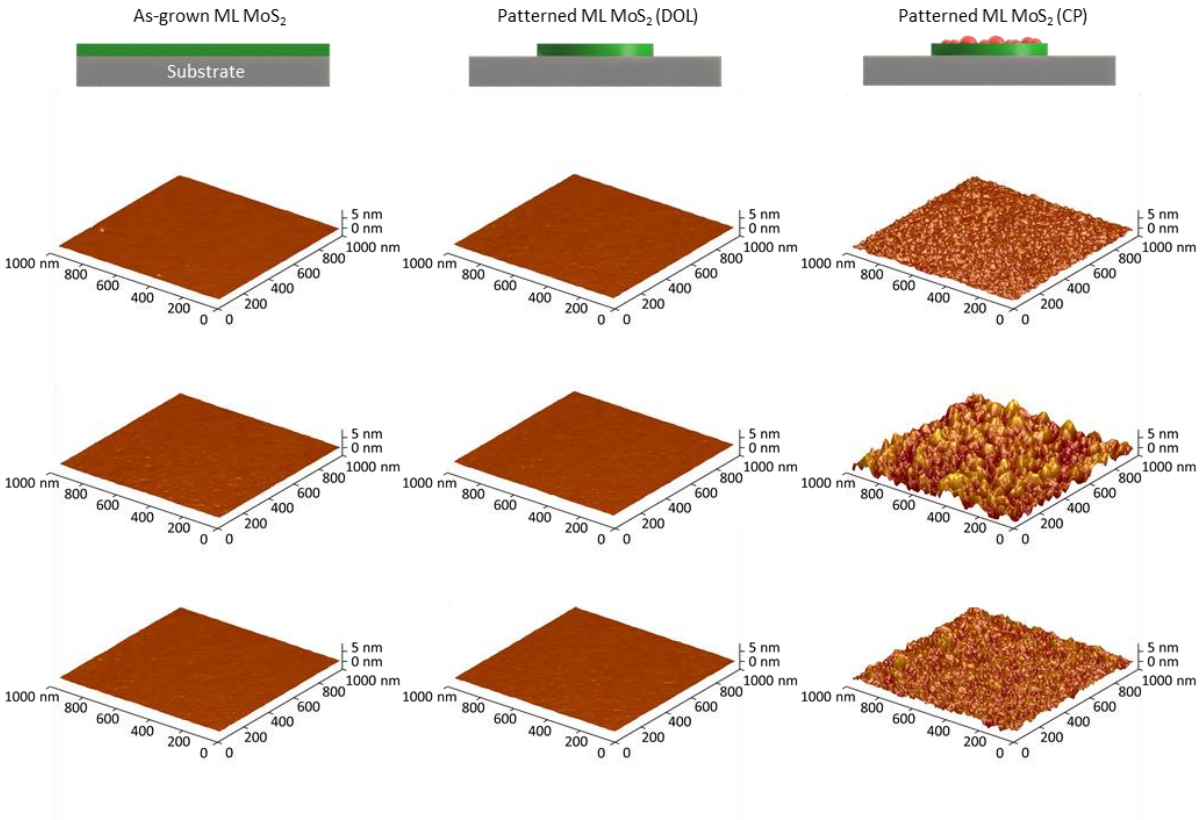

Figure S7. Multipoint AFM data for as-grown, DOL, and CP MoS_2.

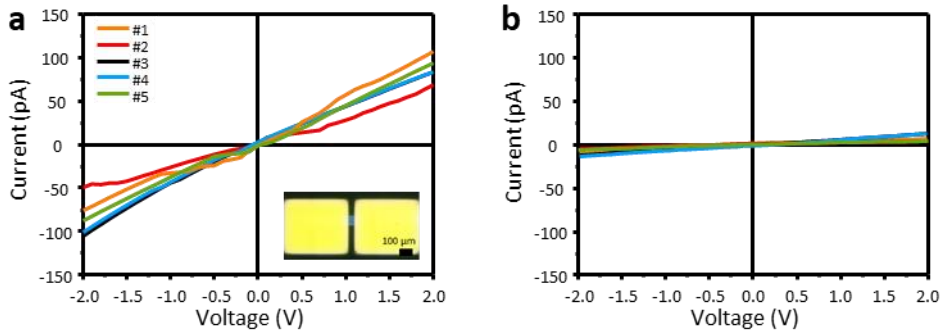

Figure S8. *I*−*V* curves of two-terminal devices with DOL (**a**) and CP BL MoS_2 (**b**). The inset image in Figure S8a indicates the OM image of two-terminal device.

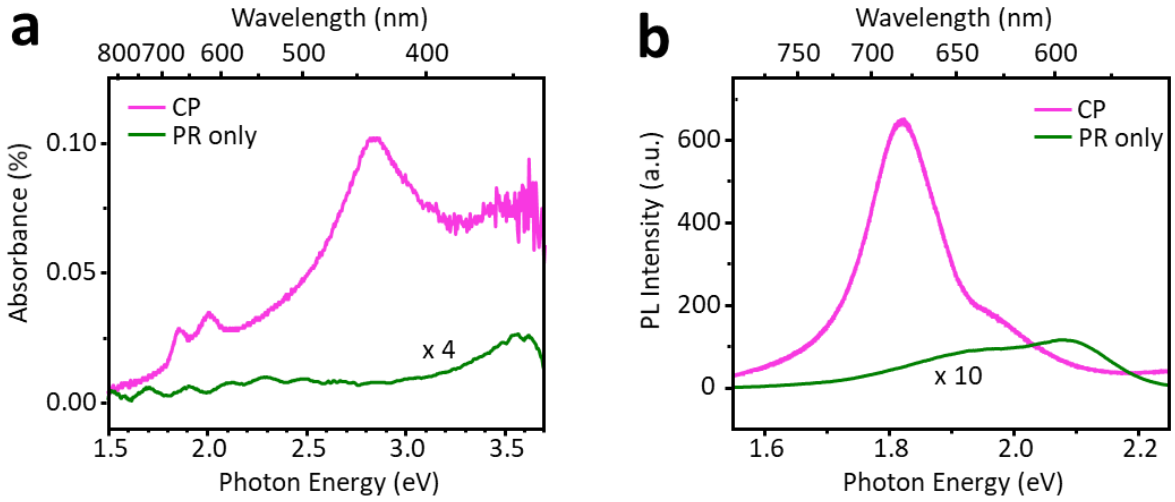

Figure S9. Optical properties of CP MoS_2 and Photoresist film on Quartz. **a**, Absorption spectra with spatially filtered broadband light source. Broad absorption peak position (~ 3.5 eV) shown in CP MoS_2 is identical to that of the photoresist film sample. **b**, PL spectra with 532 nm laser excitation. Photoresist also shows PL peak in a range of 1.9 – 2.1 eV, but it is not well-overlapped to the PL of CP MoS_2: Therefore, most of PR residues are removed and the side peak at 2.0 eV is intrinsic emission, especially B exciton. B exciton emission increases when non-radiative recombination increases.[s7]

[s7] M. M. Kathleen, T. H. Aubrey, V. S. Saujan, T. J. Berend, *APL Mater.* **2018**, 6 111106.

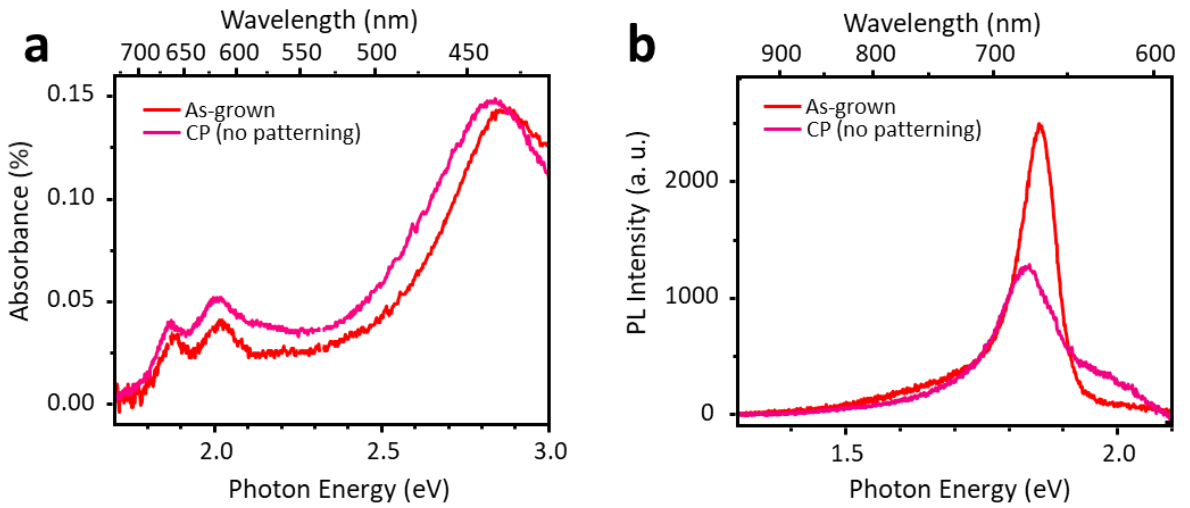

Figure S10. **a**,**b**, Micro-absorption (**a**) and PL spectra (**b**) of ML MoS_2 before and after CP process (without patterning) at the same region. Although we controlled some conditions to remove possible variations from the convolution of strain relaxation or sample-to-sample, absorption still shows redshift and PL intensity decrease with 2.5 times amount.

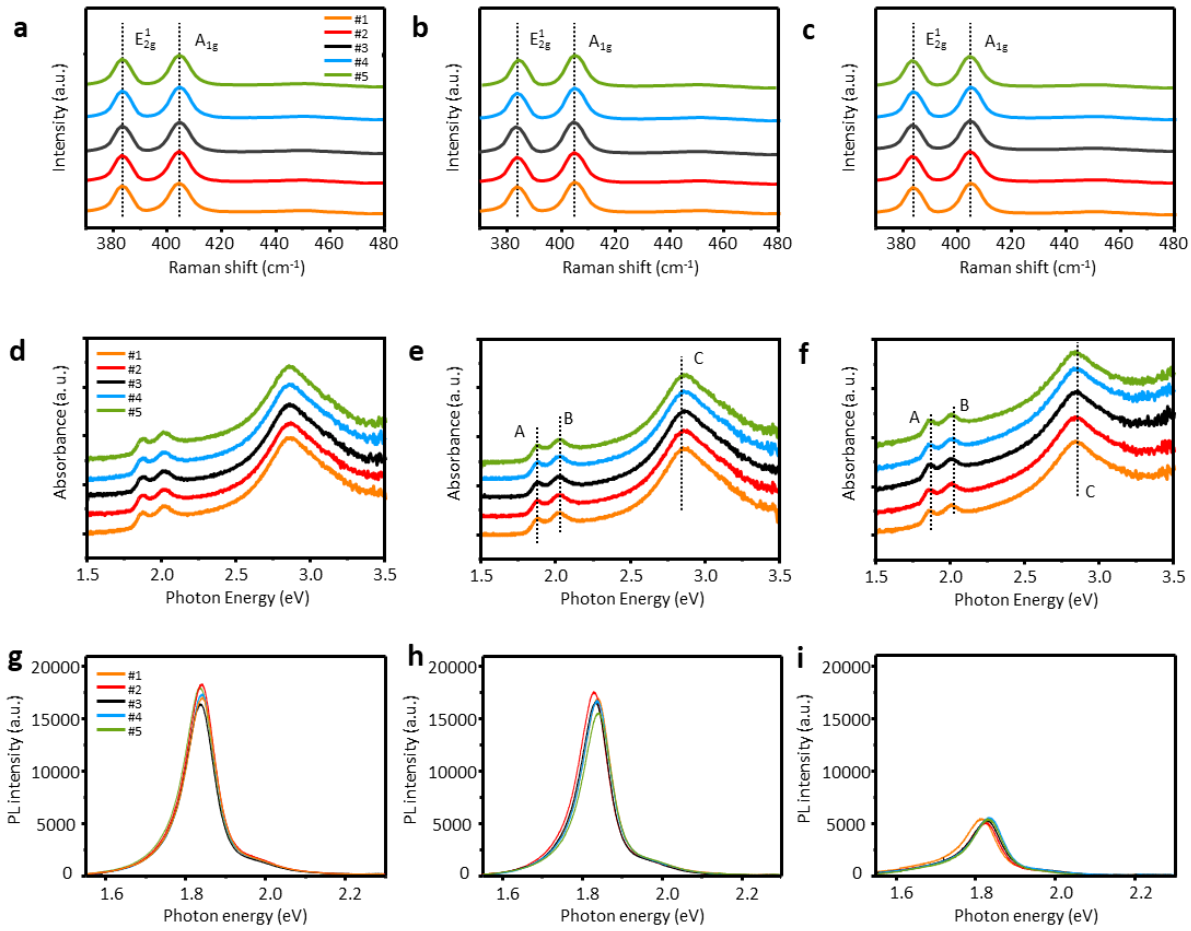

Figure S11. **a**, **b**, **c**, Raman spectra of multipoint spots in as-grown (**a**), DOL (**b**), and CP (**c**) MoS_2 with dotted lines indicating E^1_{2g} and A_{1g} peaks of as-grown MoS_2. **d**, **e**, **f**, Absorption spectra of multipoint spots in as-grown (**d**), DOL (**e**), and CP (**f**) MoS_2 with dotted lines indicating A, B, and C exciton peaks of as-grown MoS_2. **g**, **h**, **i**, PL spectra of multipoint spots in as-grown (**g**), DOL (**h**), and CP (**i**) MoS_2.

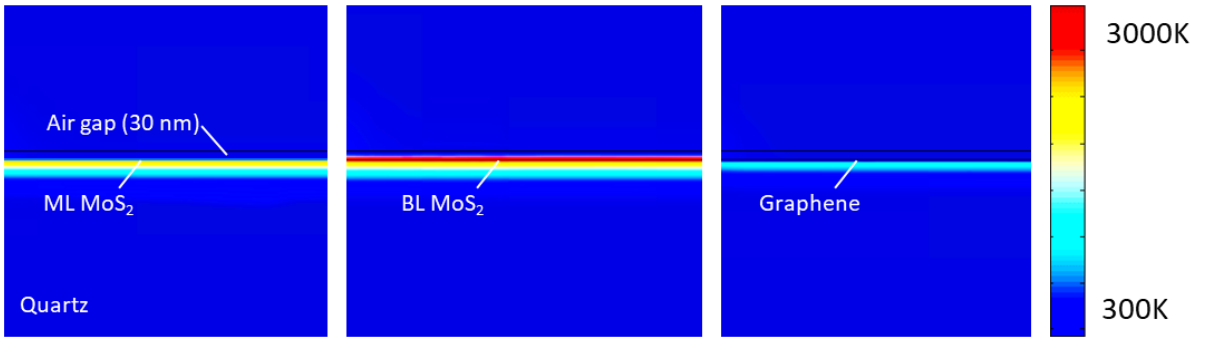

Figure S12. Cross sectional images of heat transport behaviors of ML MoS_2, BL MoS_2, and graphene on a quartz substrate in under the illumination.

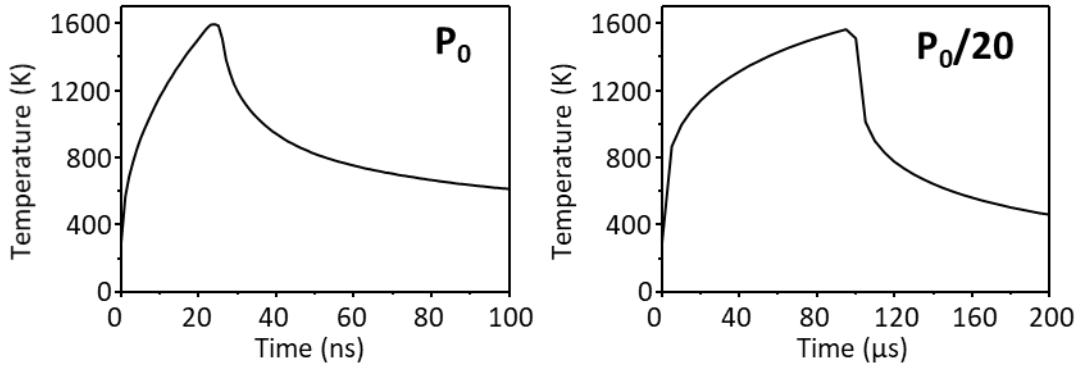

Figure S13. Time vs temperature plot of ML MoS_2 on a quartz substrate under P_0 and $P_0/20$.

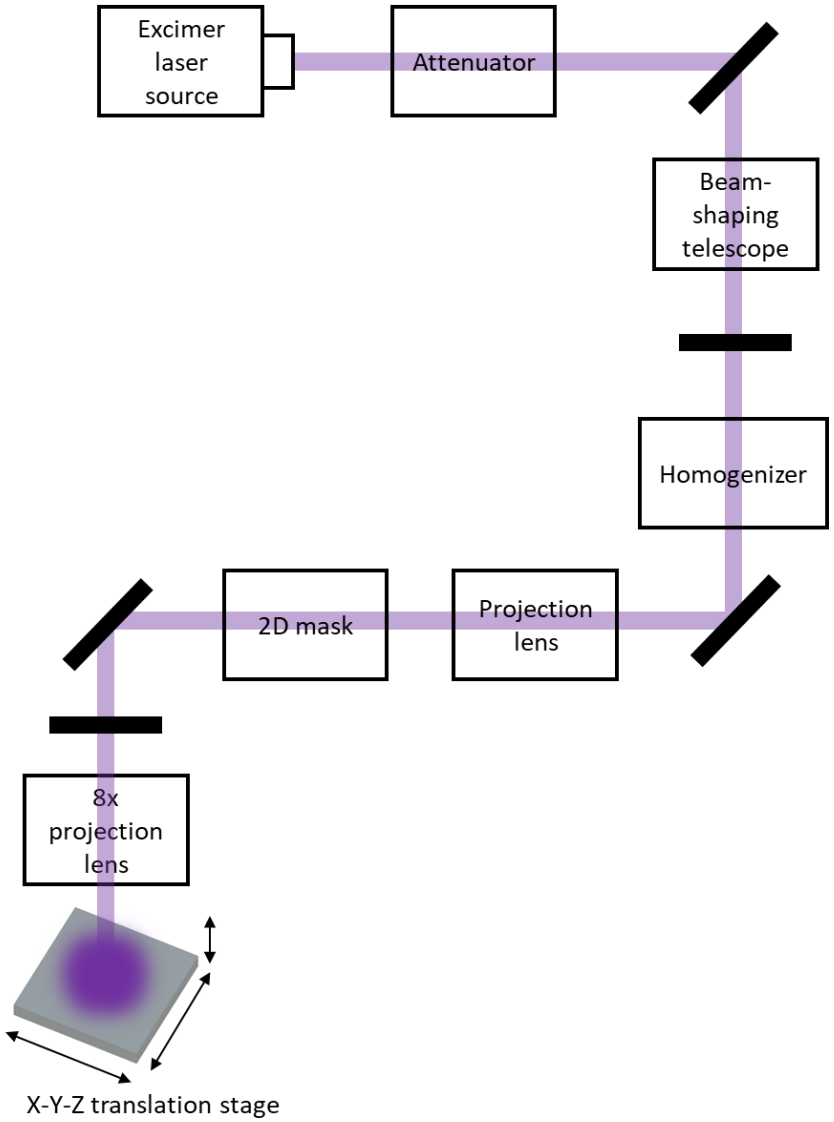

Figure S14. Schematic illustration of the excimer laser system in this work.